

**UC Berkeley**  
**SEMM Reports Series**

**Title**

Lateral Displacement Ductility of Reinforced Concrete Flat Plates

**Permalink**

<https://escholarship.org/uc/item/6f9905m8>

**Authors**

Pan, Austin  
Moehle, Jack

**Publication Date**

1987-09-01

REPORT NO.  
UCB/SEMM-87/06

STRUCTURAL ENGINEERING  
MECHANICS AND MATERIALS

**LOAN COPY**

PLEASE RETURN TO  
NISEE/Computer Applications  
404A Davis Hall  
(415) 642 - 5113

**LATERAL DISPLACEMENT DUCTILITY  
OF REINFORCED CONCRETE  
FLAT PLATES**

BY

AUSTIN PAN

AND

JACK P. MOEHLE

SEPTEMBER 1987

DEPARTMENT OF CIVIL ENGINEERING  
UNIVERSITY OF CALIFORNIA  
BERKELEY, CALIFORNIA

LATERAL DISPLACEMENT DUCTILITY OF  
REINFORCED CONCRETE FLAT PLATES

by

Austin Pan  
Graduate Research Assistant  
University of California at Berkeley

and

Jack P. Moehle  
Associate Professor of Civil Engineering  
University of California at Berkeley

September 29, 1987

## INTRODUCTION

In design of buildings to resist earthquake ground motions, the prevailing ductile design philosophy typically requires that elements of the structural system be capable of deforming into the inelastic range. This requirement often, but not always, extends to elements that are not considered in design as part of the lateral load resisting system. For example, a common form of construction in seismic zones in the United States combines flat-plate frames, to carry gravity loads, and shear walls, to resist the earthquake loads. It is unclear in this form of construction whether the flat-plate connection will possess sufficient lateral displacement capacity to survive the lateral deformations that can reasonably be expected during a strong earthquake.

The objective of this paper is to examine the available data, and therefrom develop an understanding of the major parameters that influence the lateral displacement capacity and ductility of reinforced concrete flat plates. The significant effects of gravity load and biaxial lateral loading are presented. Implications of the findings with regard to seismic design and performance are discussed.

## REVIEW OF EXPERIMENTAL OBSERVATIONS

Experimental data from several research investigations reported in the literature were gathered for this study.

Included are data from Ghali et. al. [3], Islam and Park [4], Hanson and Hanson [5], Morrison and Sozen [2], Hawkins et. al. [1], Symonds, et. al. [10], Zee and Moehle [6], and recent tests conducted by the authors (Appendix I). Prerequisites for selection of these data were: (1) specimens represented interior connections, (2) specimens contained no slab shear reinforcement, and (3) specimens were loaded to simulate effects of shears and moments due to vertical and lateral loads. Some of the specimens [Spec. No. 1-11, 15-21] were subjected to reversed cyclic lateral loads simulating severe seismic loading. Others [Spec. No. 12-14, 22-23] were subjected to effectively monotonic lateral loading.

Relevant data of these experiments are tabulated in Table 1. Brief descriptions of the specimens, test procedures, and principal results follow. More detailed information can be found in the original papers [1-6,10]. Appendix I provides details of recent tests by the authors [Spec. No. 16-19] that have not been reported previously in the literature.

#### Tests Description

All of the test specimens reported herein were similar in that a single interior connection sub-assembly was isolated from an idealized structure and loads were applied to simulate lateral load effects (Fig. 1). The column in each test specimen extended above and below the slab to "pinned" connections located at a point equivalent to the column midheight of an idealized building (Fig. 1). In the direction parallel to

lateral loading, the slab extended on either side to a point equivalent to midspan of the prototype slab, except for specimens No. 1-6 which extended 0.3 times the slab span. In the transverse direction, the total slab width ranged between half the longitudinal span and the full longitudinal span.

Slab gravity loads were simulated in some of the tests [Spec. No. 1-6, 10-11, 15-17, 20-21]. The procedure of adding these vertical loads varied; in some cases subsidiary weights were placed on the slab surface [Spec. No. 10-11, 15-17, 20-21], and in other cases vertical actuators applied the load [Spec. No. 1-6].

In some of the tests [Spec. No. 7-19] lateral load effects were simulated by attaching the slab edge to "roller" supports and then loading laterally at the top of the column (Fig. 1a). In the other tests lateral load effects were simulated by actuators that applied equal and opposite vertical loads to the ends of the slab while the columns were restrained against lateral displacement (Fig. 1b). There is no general agreement as to which of these two testing techniques is more representative of actual conditions. Both probably represent situations to which a redundant, nonlinear building system is exposed.

All tests reported previously in the literature have considered only uniaxial lateral loadings. The tests by the authors [Spec. No. 16-19] considered both uniaxial and biaxial lateral loadings as reported in Appendix I.

#### Lateral Load-Displacement Relations

For those specimens that were tested by laterally displacing the upper column [Spec. No. 7-19], the lateral load-displacement relation is self-evident from measured lateral loads and displacements at the top of the upper column. For the specimens that were loaded by vertically displacing the slab ends [Spec. No. 1-6, 20-23], the lateral load (reaction at the upper column) was resolved by statics. Lateral displacement of the specimen,  $D_h$ , was taken as

$$D_h = D_v(h_c/l_1) \dots\dots\dots (1)$$

in which  $D_v$  = difference of the vertical displacements at opposite ends of the slab at the point of vertical load application,  $h_c$  = total column height, and  $l_1$  = total span of the slab in the direction of lateral loading (Fig. 1). For the specimens No. 1-6 effective lateral displacements,  $D_h$ , obtained by equation (1) were further multiplied by a factor 1/0.6 because, as described in [1,10], the slab span of the specimen represents approximately 0.6 times the total span of the slab in the prototype.

Measured lateral load-displacement relations from three of the specimens that were subjected to reversed cyclic lateral loads are plotted in Fig. 2. These relations display the broad range of behaviors observed for the connections included in this study. The data in Fig. 2a reveal a relatively stable hysteretic response to lateral drifts well beyond the range of practical interest in building design. The data in Fig. 2b also reveal a stable hysteretic response, but to significantly less drift than

obtained for the specimen in Fig. 2a. Failure occurred in a relatively sudden punching shear mode after the slab reinforcement near the column had yielded. Lateral drift at failure in this case can be reasonably expected for a multistory building subjected to a intense earthquake motion [19]. Unless measures are taken to control lateral drift, this connection may not be suitable in a building designed to resist strong earthquakes. Figure 2c presents a response history that is even further curtailed by punching shear failure. The low level of lateral drift, and complete lack of apparent ductility, make this type of specimen clearly unsuitable for almost all types of buildings subject to severe earthquake loading.

It is useful to qualitatively classify responses of the specimens in Table 1 according to the response types depicted in Fig. 2. Column 8 of Table 2 lists the assigned classification, either A, B, or C, signifying behavior similar to that plotted in Fig. 2a, 2b, or 2c, respectively.

Two measures are used in this study to quantify the lateral deformation capacities of the specimens. The first measure is lateral drift  $D_h$  at failure, as a percent of specimen height  $h_c$ . Lateral drift at failure is tabulated for each specimen in column 6 of Table 2.

The second measure of deformation capacity is the lateral displacement ductility at failure. Lateral displacement ductility cannot be uniquely defined for slab-column connections because the force-displacement relation has no distinct yield point



(because yield spreads gradually across the slab transverse width [1]). To overcome the uncertainty in defining the yield displacement, an arbitrary procedure was applied. The procedure, illustrated in Fig. 3, was to first construct the envelope relation between lateral displacement and lateral load. The envelope relation was then idealized by an elasto-plastic relation (Fig. 3). The initial slope of the idealized relation is a secant through the measured relation at a load equal to two-thirds of the measured strength. The plastic portion of the idealized relation passes through the maximum load and the maximum deformation at failure. The intersection between these two lines defines an effective yield displacement. Displacement ductility is then calculated as the ratio between the ultimate displacement and yield displacement ( $\mu = D_u/D_y$ ) of the idealized relation (Fig. 3). The computed lateral displacement ductilities ( $\mu$ ) for the test specimens are listed in column 5 of Table 1.

#### THE EFFECT OF GRAVITY LOAD ON LATERAL DISPLACEMENT DUCTILITY

The level of gravity load carried by the slab is a primary variable affecting the apparent lateral ductility. This phenomenon has been identified in earlier tests by Kanoh and Yoshizaki [13]. The same trend is apparent in the relations plotted in Fig. 2. In that figure, lateral displacement ductility decreases from Fig. 2a to 2c, as gravity load carried by the slab increases (column 7, Table 2).

In order to generalize the conclusion that gravity load affects lateral displacement capacity of the connection, lateral displacement ductility, (column 5, Table 2), was plotted versus the normalized gravity shear ratio,  $V_g/V_o$  (column 7, Table 2), for each connection. The value  $V_g$  is the vertical shear acting at failure on the slab critical section defined at a distance  $d/2$  from the column face, in which  $d$  = the average slab effective depth. The quantity  $V_o$  is the theoretical punching shear strength in the absence of moment transfer, as given for these connections by Eq. 2 [14],

$$V_o = 4\sqrt{f'_c}b_o d \dots\dots\dots(2)$$

in which  $V_o$  is in pounds,  $f'_c$  = concrete compressive strength in psi, and  $b_o$  = perimeter length of the slab critical section ( $b_o$  and  $d$  have in. units.)

The relation between lateral displacement ductility,  $\mu$ , and the gravity shear ratio,  $V_g/V_o$ , is plotted in Fig. 4. Clearly, for values of  $V_g/V_o$  exceeding approximately 0.4 there is virtually no lateral displacement ductility ( $\mu=1.0$ ), that is, the connection fails by punching before any yield in the load-displacement relation is detected. As gravity shear decreases, there is an increase in the available ductility.

The effect of gravity shear on lateral drift at failure is presented in Fig. 5. As in Fig. 4, there is a reduction in available drift with increasing gravity shear ratio.

The observation that lateral deformation capacity and gravity shear are related also is not surprising, and has been

identified previously [1,4]. According to the ACI Building Code [7] shear strength for square interior columns is defined by Eq. 2. This limiting shear strength has been established from test of slab-column connections for which shear failure occurred before widespread yielding of the slab reinforcement [9]. The condition for which this limiting shear stress is defined is consistent with the philosophy of the main body of the ACI Building Code, namely, that design loads are set sufficiently high and inelastic redistribution is sufficiently limited that significant yield at connections will not occur. Under this loading condition, the surrounding slab confines the connection region. This confinement is believed to be the reason why observed nominal shear stresses at failure are larger for slab-column connections than for linear elements such as beams [14]. Some researchers [9] have hypothesized that the confining effect of the slab is diminished when widespread yield of the slab reinforcement occurs in the connection region. Experimental data in support of this hypothesis have been presented previously [9] for connections loaded solely by vertical loads. The data for lateral load tests presented in Fig. 4 augment these vertical load data.

#### THE EFFECT OF BIAXIAL LATERAL LOADING ON LATERAL DISPLACEMENT DUCTILITY

During wind or earthquake loading, the slab-column connection resists lateral loads acting in multiple directions.

To investigate the influence of biaxial lateral loading, four specimens were tested. Limited details of the tests are presented for reference in Appendix I. In the test program, two specimens were tested with a uniaxial lateral displacement history, one with "high" gravity load (AP1), and one with relatively "low" gravity load (AP3). Nominally identical specimens (AP2 and AP4) were subsequently subjected to biaxial lateral load histories. The displacement histories are compared in Fig. 6. The biaxial load history followed sequentially the points 1 through 14 indicated in Fig. 6.

Figures 7 and 8 show the measured relations between lateral force and lateral drift. As can be observed in those figures, the biaxially loaded specimens (AP2 and AP4) failed at an earlier stage of testing in comparison with the companion uniaxially-loaded specimens. Both stiffness and strength were less for the biaxially-loaded specimens than for the equivalent uniaxially loaded specimens.

The lower resistance and toughness of the biaxially loaded specimens is explained as follows. Under uniaxial loading, resistance is attributable to torsion on faces AB and CD and shear and moment on faces BC and DA [1] (Fig. 9). If a uniaxially loaded connection is subsequently loaded in the transverse direction, faces AB and CD (which had previously been loaded in torsion) begin to develop flexure and shear, while faces BC and DA (which had previously been loaded in moment and shear) begin to develop torsion. The interaction between flexure, shear and

torsion [11] are such that the net connection resistance in any given direction is less under biaxial loading than under uniaxial loading. Similarly, more rapid degradation of the concrete occurs under biaxial loading.

Based on the observations from this series of tests, it is concluded that biaxial lateral loading, as might occur during an earthquake or wind loading, reduces the available strength, stiffness, and overall lateral displacement capacity of slab-column connections. Thus, since most of the data included in Fig. 4 and 5 were obtained from uniaxial tests, conclusions drawn therefrom may be on the unconservative side if biaxial loading occurs.

#### IMPLICATIONS OF THE TEST RESULTS

The data in Fig. 4 and 5 indicate that the available lateral displacement ductility of reinforcement concrete flat-plate connections without shear reinforcement is low by comparison with values often considered marginally acceptable in seismic design [11]. However, the existence of low ductility does not de facto equate with poor performance during a strong earthquake loading. For typical slab-column connections, relatively high flexibility may protect the connection from large displacement ductility demands. For example, Fig. 10 presents idealized load displacement envelopes of a typical slab-column connection [6] and a slender shear wall [23] that might be used to stiffen a flat-plate building. If the wall is sufficiently stiff to

restrain lateral interstory drifts to approximately 1.5 percent of story height (a value occasionally quoted as a reasonable upper bound for severe seismic loading [20]), the required displacement ductility of the wall will be approximately six. The required displacement ductility of the slab-column connection will be less than two.

According to the data presented in Fig. 4 and 5, a slab-column connection can be expected to possess some minimal ductility, and a drift capacity of at least 1.5 percent of interstory height, only if the vertical shear on the connection is less than or equal to approximately 40 percent of the direct punching shear strength. Expressed in terms of shear stresses, the nominal shear stress due to vertical loads should be limited to approximately  $(0.4)(4\sqrt{f'_c}) \sim 1.5\sqrt{f'_c}$  psi on the slab critical section. The vertical load should be taken at least equal to the design gravity load shear. Although it is likely that vertical accelerations during earthquakes (frequently of the same magnitude as the lateral ground accelerations) will further increase the total connection shear, there is no evidence at the present time to prove that this effect should be included when computing the vertical connection shear. Likewise, there is no evidence to confute this possibility.

If gravity loads alone are considered in computing the proposed limiting shear stress, the minimum required column size to satisfy the recommendation is approximately 19x19 in. for a building slab having 20-foot bays, an eight inch slab, 15 psf

superimposed dead load, 40 psf service live load, and 4000-psi concrete normal weight concrete. Supporting calculations are in Appendix II.

For lateral interstory drifts exceeding 1.5 percent of interstory height, adequate performance of the flat-plate cannot be assured. For this reason, a suitable structural system should be provided to limit lateral drifts.

#### SUMMARY AND CONCLUSIONS

Experimental data from several investigations are analyzed to identify the parameters that influence the lateral displacement ductility of reinforced concrete flat-plate connections subjected to lateral loads. Only interior, conventionally-reinforced slabs without slab shear reinforcement are considered. Implications of the findings are discussed. The following main conclusions are recapitulated:

1. The magnitude of the gravity load shear carried by the slab is a primary variable affecting the lateral displacement capacity and ductility.

2. For a given level of gravity load, biaxial lateral loading reduces lateral load stiffness, strength, and available ductility.

3. The magnitudes of gravity loads and of lateral interstory drifts should be controlled to ensure that integrity of the slab-column connection is maintained under seismic loading. Lateral interstory drifts under an extreme earthquake

loading should not exceed 1.5 percent of interstory height. At this level of deformation, the available data indicate that the flat-plate connection will perform adequately if the gravity level shear stress acting on the slab critical section does not exceed  $1.5\sqrt{f'_c}$ .

#### NOTATION

- $A_c$  = cross section area of slab critical section.
- $b_o$  = perimeter of critical section for slab, in.
- $c_1$  = column dimension in direction of loading, in.
- $c_2$  = column dimension transverse to direction of loading, in.
- $D_h$  = horizontal displacement at top of column. See Fig. 1a.
- $D_u$  = ultimate displacement at failure.
- $D_v$  = difference of the vertical displacement at opposite ends of the slab. See Fig. 1b.
- $D_y$  = yield displacement.
- $d$  = distance from extreme compression fiber to centroid of tension reinforcement, in.
- $d_{avg}$  = average  $d$ , in.
- $h$  = overall thickness of slab, in.
- $h_c$  = column height.
- $f'_c$  = concrete compression strength, psi.
- $f_y$  = steel yield strength, psi.
- $l_1$  = span length in direction of lateral load.
- $l_2$  = span length transverse to direction of lateral load.
- $V_g$  = shear due to gravity loads including self weight, kips.
- $V_{all}$  = allowable shear stress.



$V_o$  = theoretical punching shear strength Eq. 2.  
 $w_g$  = dead load.  
 $w_l$  = live load.  
 $w_{sdl}$  = superimposed dead load.  
 $w_{slab}$  = slab self weight.  
 $\mathcal{M}$  = displacement ductility. =  $D_u/D_y$

#### APPENDIX I - TESTS WITH BIAXIAL LOADING

To investigate the influence of biaxial loading on connection behavior, four tests were conducted in 1986 by the authors at the University of California at Berkeley. A brief summary of the experimental program follows.

##### Specimen Description

Four identical interior connections were constructed as shown in Figure (A.1). Slab dimensions were 13 ft by 13 ft with a thickness of 4.8 inches. Column dimensions were 10.8 inches by 10.8 inches in cross section extending 3 ft. above and below the slab. Concrete compression strength was specified at 4,000 psi. Slab reinforcement was all No. 3 Grade 60 reinforcing bars. The column was heavily reinforced to ensure failure of the slab connection. The slabs were similar in design to those tested previously by Moehle and Diebold (21) and by Zee and Moehle (6).

##### Experimental Setup

To allow for bi-directional movement, the edges of the slab were supported by steel transducer struts fitted with universal bearings at both ends. The top and bottom of the column were also

fitted with universal bearings (Fig. A.1). At the west end of the slab a torsional restraining frame was attached to reduce in-plane rigid body twisting during testing. Two hydraulic load actuators were connected at the top of the column for lateral loading. Gravity load was simulated and maintained at a constant value by adding lead blocks on the slab and by jacking up the bottom of the column. The specimen was instrumented to measure deflections, slab rotations and profiles, reinforcement strains, and secondary displacements.

#### Test Sequence

To investigate the influence of gravity load on connection behavior, high gravity load ( $0.35V_0$ ) was imposed on specimens AP1 and AP2, and low gravity load ( $0.18V_0$ ) was imposed on specimens AP3 and AP4. Specimens AP1 and AP3 were tested with uniaxial lateral load. Tests of specimens AP2 and AP4 were biaxial. Figure 6 shows the cyclic displacement sequence for the uniaxial tests. The biaxial tests adopted the same sequence but applied in a "clover leaf" pattern from points 1 through 14 of the diagram illustrated in Fig. 6. Plots of lateral force versus drift are shown in figures 7 and 8 for the four specimens.

APPENDIX II - Sample Calculation of Minimum Required Column Size.

Given :  $h = 8'$ ,  $l_1 = l_2 = 20'$ ,  $f'_c = 4000$  psi,  $w_{sd1} = 15$  psf,  $w_1 = 40$  psf

Find : Minimum required column size to ensure drift capacity of 1.5 % and lateral displacement ductility of two.

$$d = h - 1.0 = 7 \text{ in.}$$

$$w_{\text{slab}} = (8/12) \times 150 = 100 \text{ psf}$$

$$w_u = 0.75(1.4D + 1.7L + 1.7(1.1E)) \\ = 0.75(1.4(100 + 15) + 1.7(40)) = 171.75 \text{ psf}$$

$$V_g = 171.75 \times 20 \times 20 = 68700 \text{ lb}$$

$$v_{\text{all}} = 1.5 \sqrt{f'_c} = 94.9 \text{ psi}$$

$$A_c = V_g / v_{\text{all}} = 68700 / 94.9 = 723.9 \text{ in}^2$$

$$b_o = A_c / d = 723.9 / 7 = 103.4 \text{ in.}$$

$$b_o / 4 = 25.9 \text{ in. (Assuming square column)}$$

$$c_1 = 25.9 - d = 18.9 \text{ in. Say } \underline{19 \text{ inches}}$$

#### APPENDIX III-REFERENCES

1. Hawkins, N. M., Mitchell D., and Sheu M. S., "Cyclic Behavior of Six Reinforced Concrete Slab-Column Specimens Transferring Moment and Shear," Progress Report 1973-74 on NSF Project GI-38717, Section II. Dept. of Civil Engineering, University of Washington, Seattle, WA, 1974.
2. Morrison, D. G., Sozen, M. A., "Response of Reinforce concrete Plate-column Connections to Dynamic and Static Horizontal Loads," Civil Engineering Studies, Structural Research Series No. 490, University of Illinois at Urbana-Champaign, Urbana, Illinois, April, 1981.
3. Ghali, A., Elmasri, M. Z., and Dilger, W., "Punching of Flat Plates Under Static and Dynamic Horizontal Forces," American Concrete Institute Journal, Title No. 73-47, October, 1976, pp. 566-572.
4. Islam, S., and Park, R., "Tests on Slab-Column connections with Shear and Unbalanced Flexure," Journal of the Structural Division, ASCE, Vol.102, No. ST3, March, 1976, pp. 549-568.
5. Hanson, N. W., and Hanson, J. M., "Shear and Moment Transfer between concrete Slabs and Columns," Journal of the Portland Cement Association, Research and Development Laboratories, Vol. 10, No. 1, Jan., 1968, pp 2-16.
6. Zee, H. L., and Moehle, J. P., "Behavior of Interior and Exterior flat Plate Connections Subjected to Inelastic Load Reversals," Earthquake Engineering Research Center, Report No. UCB/EERC-84/07, August, 1984, University of California,

Berkeley.

7. American concrete Institute Committee 318, "Building Code Requirments for Reinforced Concrete," ACI 318-83, Detroit, Michigan, 1983, 102 pp.
8. Moment, shear, torsion interaction reference.
9. Hawkins, N. M., and Mitchell, D., "Progressive collapse of Flat Plate Structures," American Concrete Institute Journal, Vol. 76, No. 7, July 1979, pp. 775-808.
10. Symonds, D. W., Mitchell, D., and Hawkins, N. M., "Slab-Column Connections Subjected to High Intensity Shears and Transferring Reversed Moments" Progress Report on NSF Project GI-38717, Dept. of Civil Engineering, University of Washington, Seattle, WA, August, 1976.
11. Park, R., and Pauley, T., "Reinforced Concrete Structures," John Wiley & Son, 1975, 769 p.
12. Hawkins, N. M., "Shear and Moment Transfer Between Concrete Flat Plates and Columns," Progress Report on NSF Grant No. GK-16375, Dept. of Civil Engineering, University of Wahsington, Seattle, 1971.
13. Kanoh, Y., and Yoshizaki, S., "Experiments on Slab-Column and Slab-Wall Connections of Flat Plate Structures," Concrete Journal, Japan Concrete Institute, Vol. 13, June, 1975, pp. 7-19.
14. ASCE-ACI Committee 426, "The Shear Strength of Reinforced Concrete Members - Slabs," Journal of the Structural Division, ASCE, Vol. 100, No. ST8, August 1974, pp. 1543-1591.
15. Moe, J., "Shearing Strength of Reinforced Concrete Slabs and Footings under Concentrated Loads," Development Department Bulletin D47, Portland Cement Association, April 1961, 130pp.
16. Carpenter, J. E., Kaar, P. H., and Corley, W. G., "Design of Ductile Flat Plate Structures to Resist Earthquakes," Proceedings of the 5th World Conference on Earthquake Engineering, Paper No. 250, Session 5D, Rome, Italy, 1973.
17. "Uniform Building Code," International Conference of Building Officials, Whittier, California, 1983.
18. Chopra, A. K., "Dynamics of Structures, a Primer," Engineering Monographs on Earthquake Criteria, Structural Design, and Strong Motion, Earthquake Engineering Research Institute, 1981.

19. Newmark, N. M., and Hall, W. J., "Earthquake Spectra and Design," Engineering Monographs on Earthquake Criteria, Structural Design, and Strong Motion, Earthquake Engineering Research Institute, 1982.
20. Sozen, M. A., "Review of Earthquake Response of Reinforced Concrete Buildings with a View to Drift Control," State-of-the Art in Earthquake Engineering, Seventh World Conference on Earthquake Engineering, Istanbul, 1980, pp.119-174.
21. Moehle, J. P., and Diebold, J., "Experimental Study of the Seismic Response of a Two Story Flat Plate Structure," Earthquake Engineering Research Center, Report No. UCB/EERC-84/08, August 1984, University of California at Berkeley.
22. Vanderbilt, M. D., and Corley, W. G., "Frame Analysis of Concrete Buildings," Concrete International, Dec. 1983, pp. 33-43.
23. Hiraishi, H., Nakata, S., and Kaminosono, T., "Static Tests on Shear Walls and Beam-Column Assemblies and Study on Correlation between Shaking Table Tests and Pseudo-Dynamic Tests," Earthquake Effects on Reinforced Concrete Structures, US-Japan Research, James K. Wight, Editor, American Concrete Institute, SP-84, Detroit, 1985.

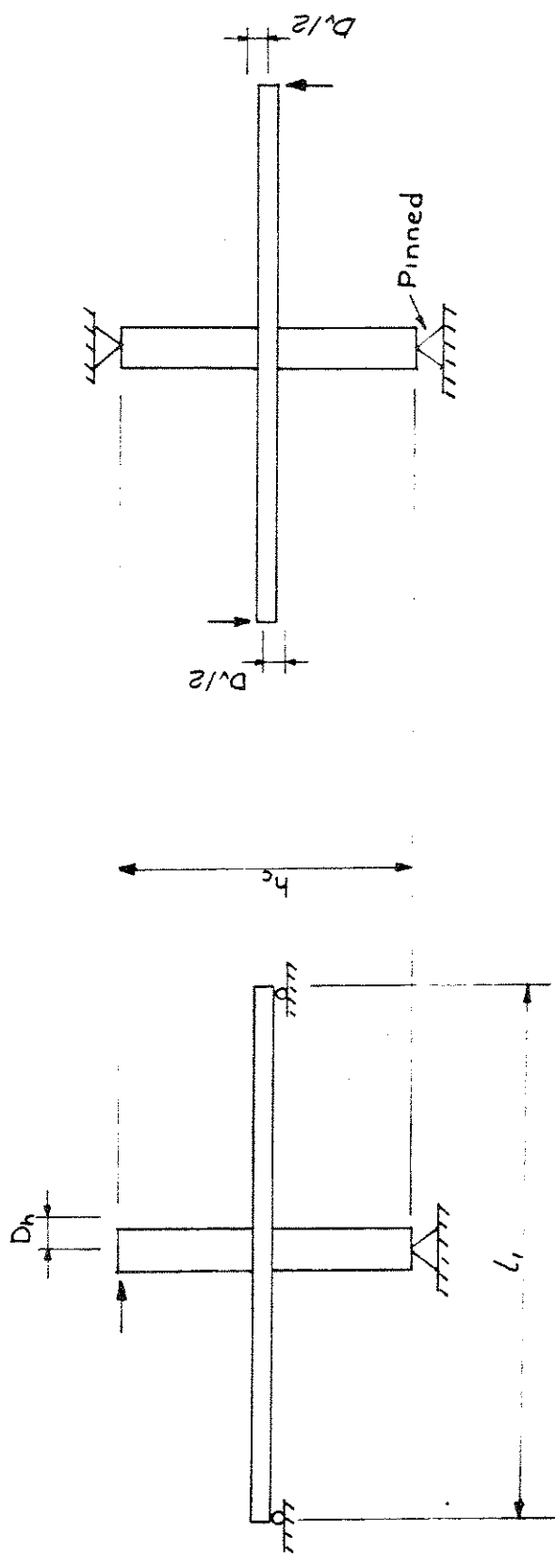
TABLE (1) - DATA ON EXPERIMENTAL SPECIMENS

1	2	3	4	5	6	7	8	9	10	11	12	13	14
Specimen Number *	Label	Researcher	cl (mm.)	cz (mm.)	h (mm.)	dava (mm.)	ll (mm.)	lr (mm.)	lc (mm.)	plcsh %	prcsh ***	f <sub>y</sub> (psi)	f <sub>u</sub> (psi)
1	S1		12	12	6	4.6	144	84	102	0.012	0.0059	66600	5030
2	S2	Hawkins	12	12	6	4.6	144	84	102	0.0084	0.0049	67100	5100
3	S3	et al	12	12	6	4.6	144	84	102	0.0055	0.004	66000	5050
4	S4		12	12	6	4.6	144	84	102	0.012	0.0059	66600	4690
5	S6	Symonds et	12	12	6	4.6	144	84	102	0.0181	0.0091	66600	3360
6	S7	al	12	12	6	4.6	144	84	102	0.0084	0.0049	67100	3840
7	S1		12	12	3	2.36	72	44	44	0.0065	0.0045	46800	6640
8	S2	Harrison	12	12	3	2.36	72	44	44	0.0098	0.0098	47900	5090
9	S3	and	12	12	3	2.36	72	44	44	0.0131	0.0131	46600	4220
10	S4	Sozen	12	12	3	2.36	72	44	44	0.0098	0.0098	46000	5060
11	S5		12	12	3	2.36	72	44	44	0.0098	0.0098	47300	5110
12	SH 0.5	Ghali	12	12	6	4.25	72	46	46	0.005	0.00167	69000	5329
13	SH 1.0	et	12	12	6	4.25	72	46	46	0.01	0.00333	69000	4835
14	SH 1.5	al.	12	12	6	4.25	72	46	46	0.015	0.005	69000	5794
15	Interio	Zee	5.4	5.4	2.9	1.60	72	32	32	0.008	0.006	63100	5400
16	AF1		10.8	10.8	4.84	4.07	144	104	72	0.0026	0.0029	70200	4250
17	AF2	Authors	10.8	10.8	4.84	4.07	144	104	72	0.0026	0.0029	70200	4400
19	AF3		10.8	10.8	4.84	4.07	144	104	72	0.0026	0.0029	70200	4620
19	AF4		10.8	10.8	4.84	4.07	144	104	72	0.0026	0.0029	70200	4500
20	IF2	Islam &	9	9	3.5	2.75	108	90	60	0.0106	0.00534	54200	4630
21	IF3C	Park	9	9	3.5	2.75	108	90	60	0.0106	0.00534	45800	4310
22	B7	Henson &	12	4	3	2.25	72	48	63	0.015	0.015	51400	4760
23	C8	Hanson	6	12	3	2.25	72	48	63	0.015	0.015	59600	4760

\* Designation used by original researchers.  
 \*\* Top steel ratio within 3h strip over column.  
 \*\*\* Bottom steel ratio within 3h strip over column.  
 Note : 1 in. = 25.4 mm

TABLE 10. NUMBER OF ABSTRACTS IN EACH CLASS

Specimen Number	Label	Researcher(s)	VC (Papers)	4	5	6	7	8
				Number	Number	Number	Number	Classification
1	S1		20.6	1.38	3.2%	0.39		D
2	S2	Hawkins	1.32	1	0.0%	0.147		C
3	S3	et al	31.2	1	0.0%	0.401		C
4	S4		33.9	1.9	2.6%	0.402		B
5	S6	Sydney	61	1	1.6%	0.861		C
6	S7	et al	61	1	1.6%	0.860		C
7	S1		1.35	3.2	1.7%	0.041		H
8	S2	Harrison	1.35	1.9	2.8%	0.035		B
9	S3	and	1.35	0.9	4.7%	0.335		H
10	S4	Sozen	2	4.2	4.5%	0.078		H
11	S5		6.46	4	4.1%	0.160		A
12	SM 0.5	Shall	29	3.6	6.0%	0.212		A
13	SM 1.0	et al	29	1.4	2.7%	0.389		D
14	SM 1.5	et al	19	1.8	2.7%	0.277		B
15	Interior	7/e	3.0	3.2	3.0%	0.202		B
16	API		78.37	1.7	1.0%	0.362		D
17	API 2	Authors	23.32	1.07	1.0%	0.363		B
18	API 3		12	2.37	4.7%	0.183		K
19	API 4		12	3.11	3.0%	0.185		B
20	IP2	Islam &	6.42	3.2	5.0%	0.112		A
21	IP3:	Farf	3.64	4	4.0%	0.225		B
22	B7	Harrison &	1.1	2.4	2.8%	0.037		B
23	C8	Harrison	1.56	2.8	5.8%	0.045		A



(a) Lateral Load at Column

(b) Vertical Load at Slab Edges

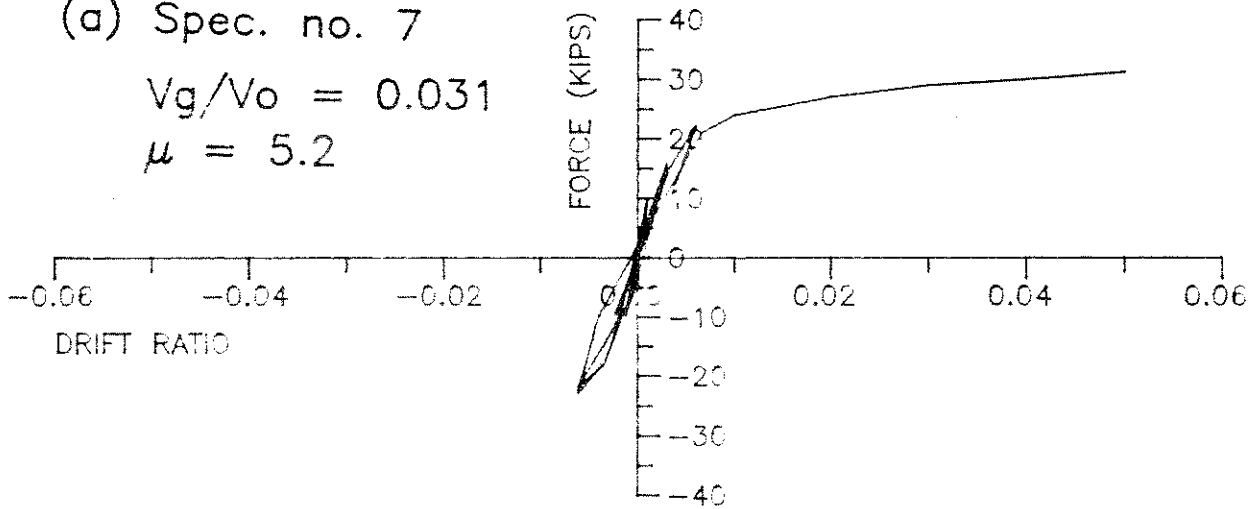
FIG. 1 - LATERAL LOAD SIMULATION



(a) Spec. no. 7

$$V_g/V_o = 0.031$$

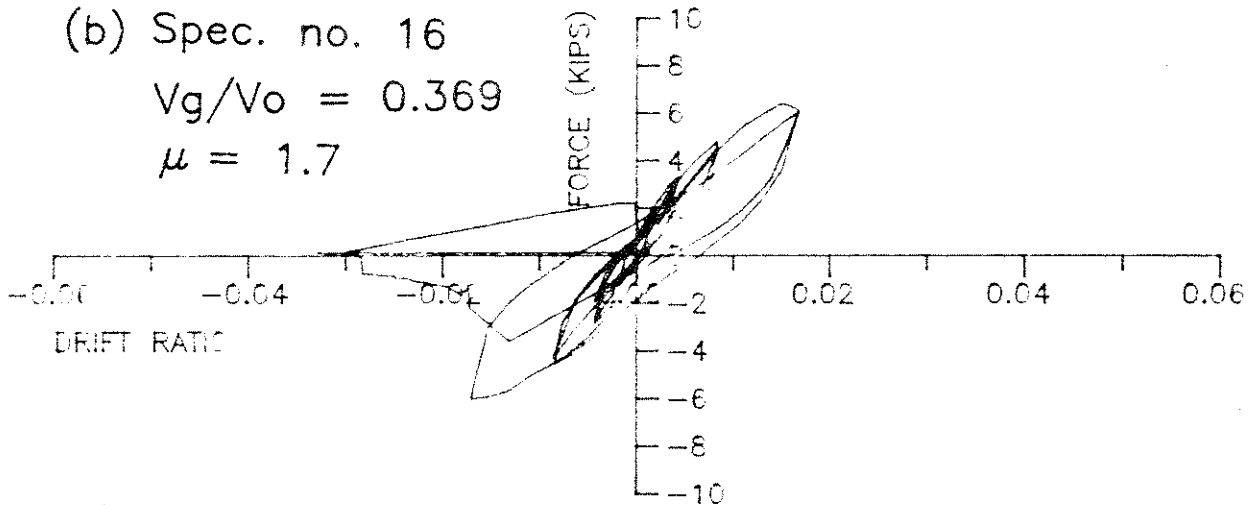
$$\mu = 5.2$$



(b) Spec. no. 16

$$V_g/V_o = 0.369$$

$$\mu = 1.7$$



(c) Spec. no. 2

$$V_g/V_o = 0.449$$

$$\mu = 1$$

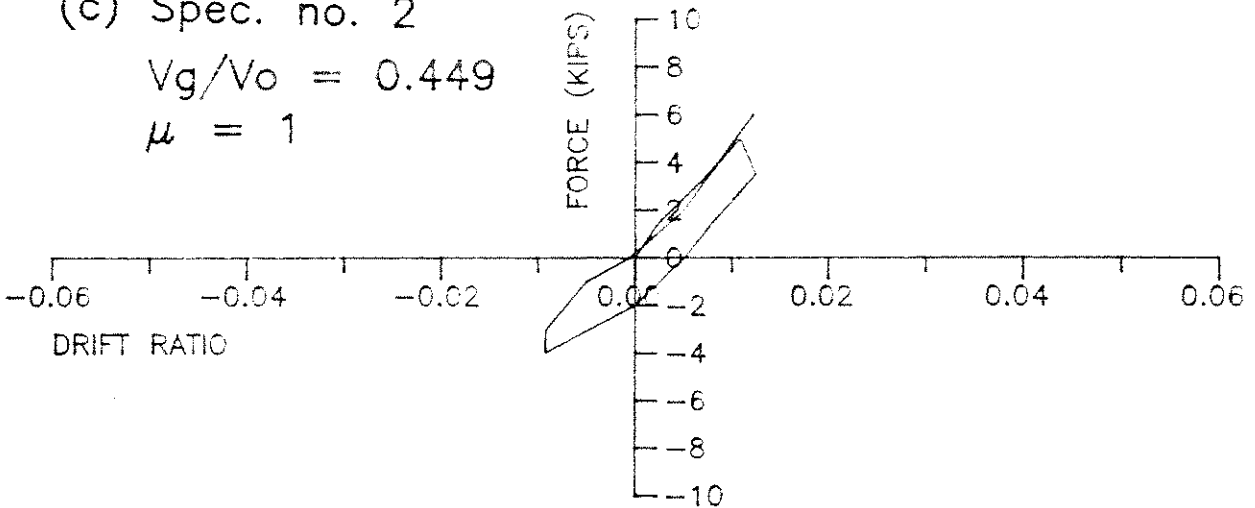


**FIG 2 - CLASSIFICATION OF SPECIMEN RESPONSE**

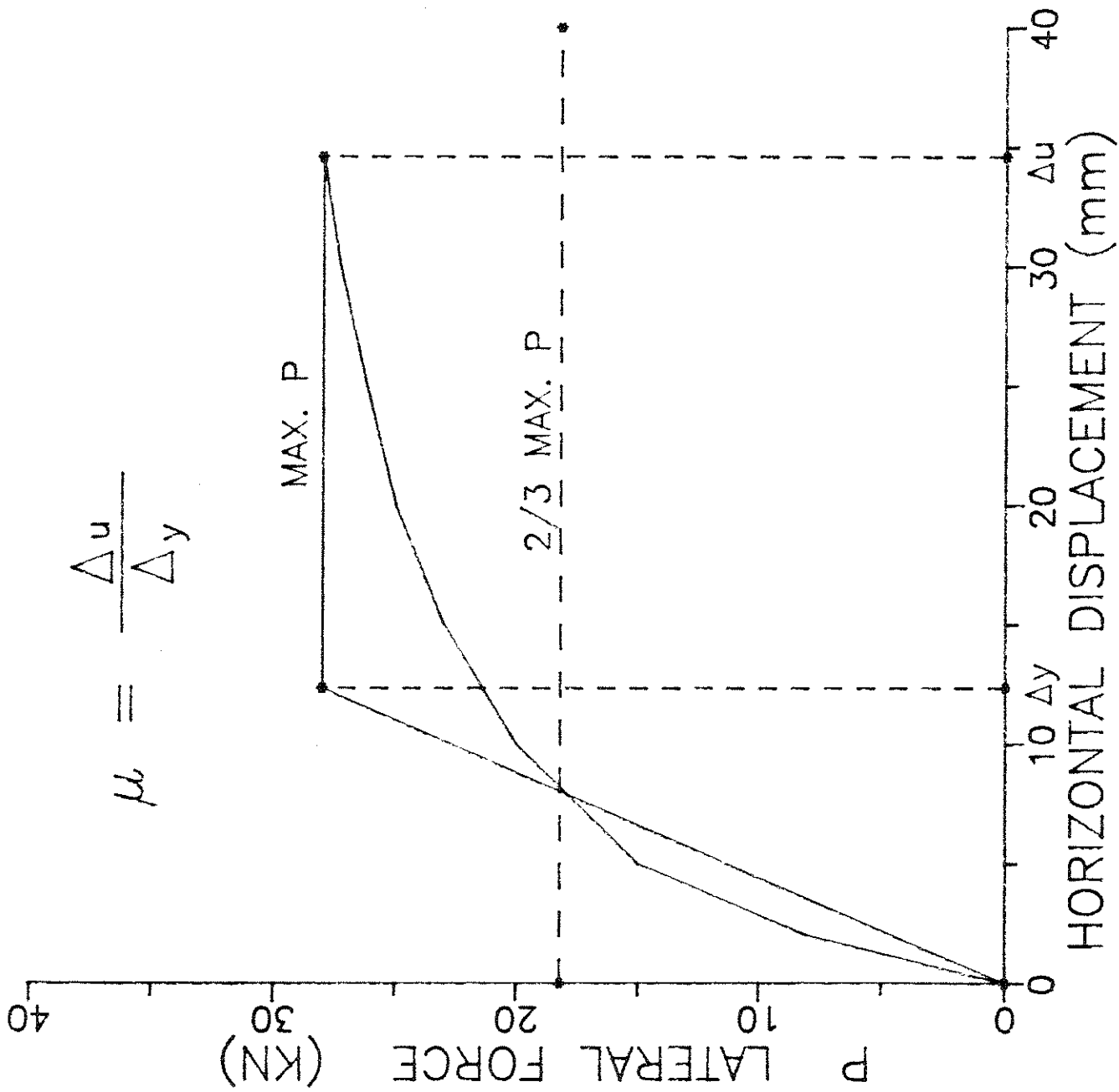
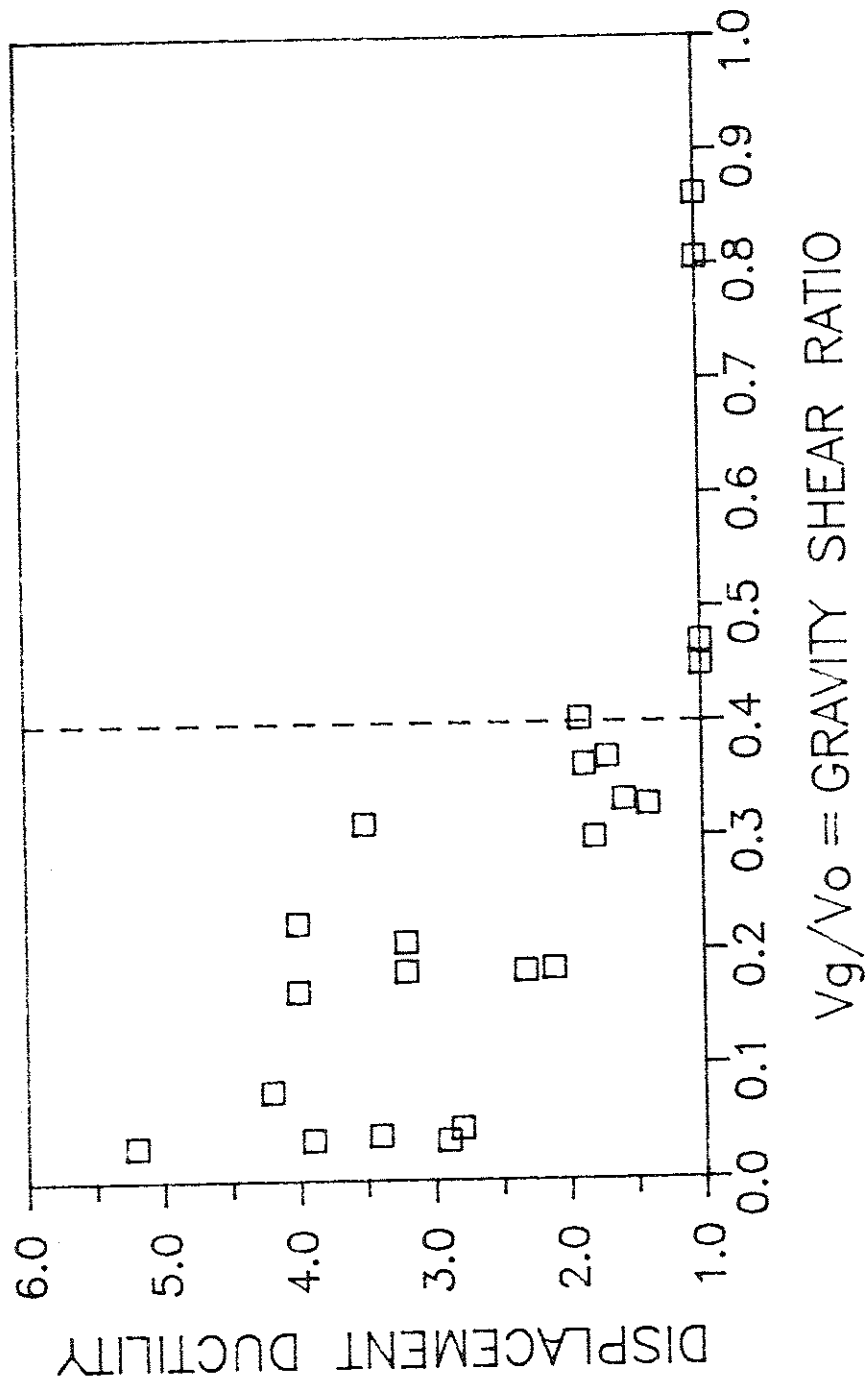
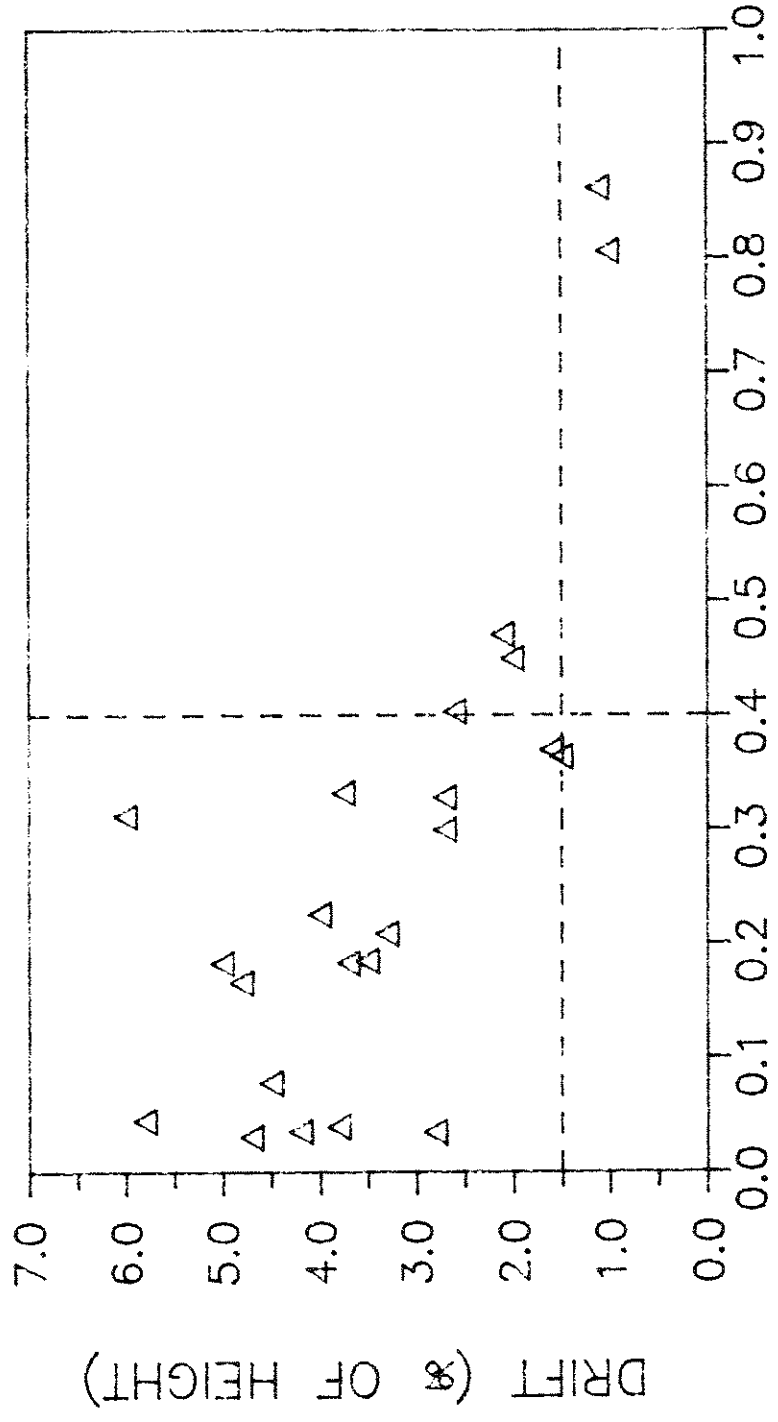


FIG. 3 - DEFINITION OF DISPLACEMENT DUCTILITY



**FIG. 4 - EFFECT OF GRAVITY LOAD ON DUCTILITY**



Vg/Vo = GRAVITY SHEAR RATIO

FIG. 5 - EFFECT OF GRAVITY LOAD ON DRIFT

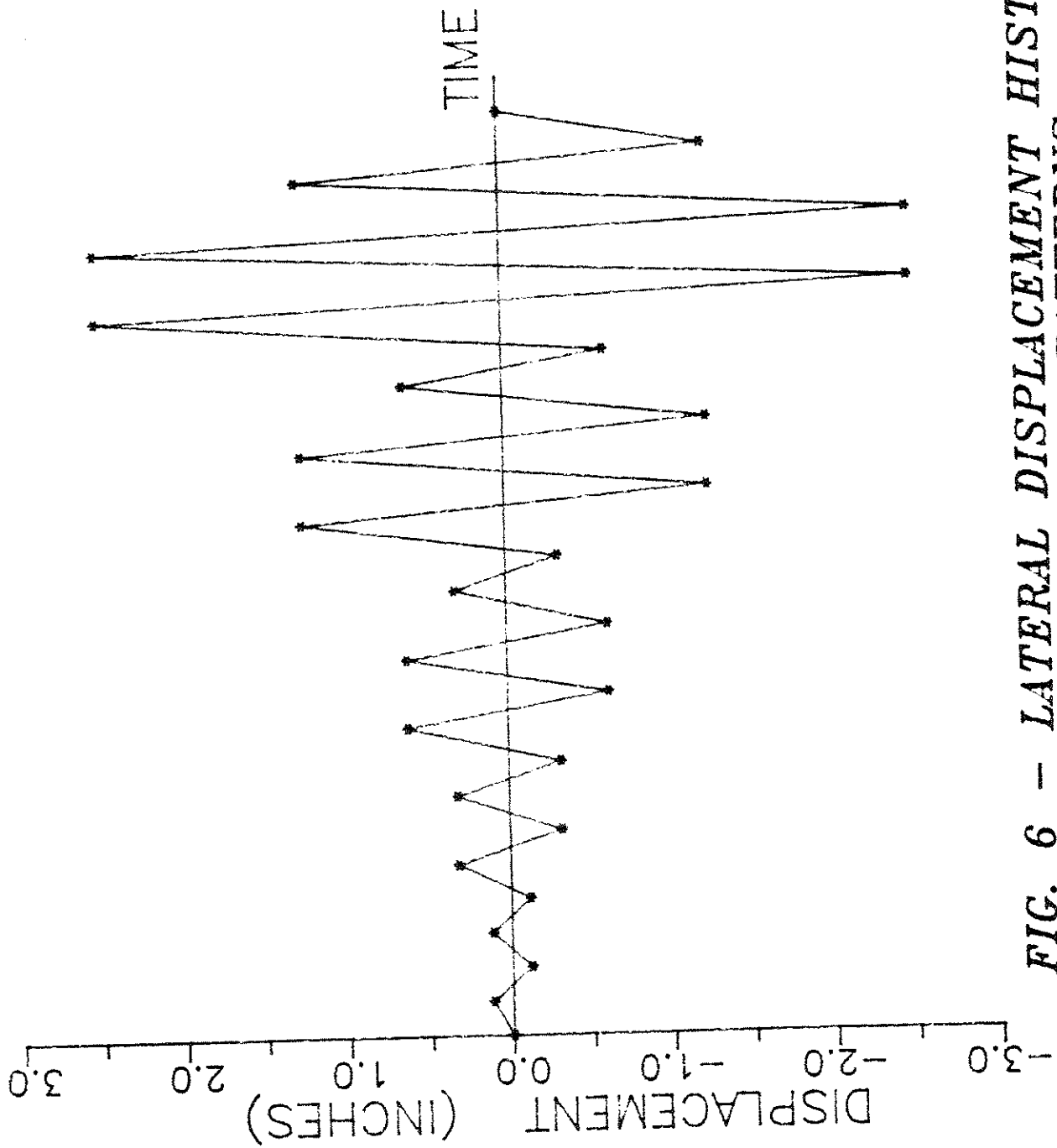
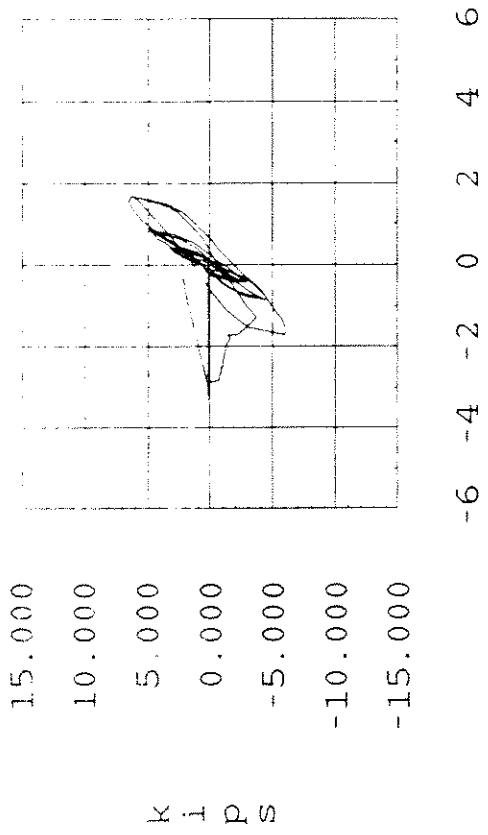
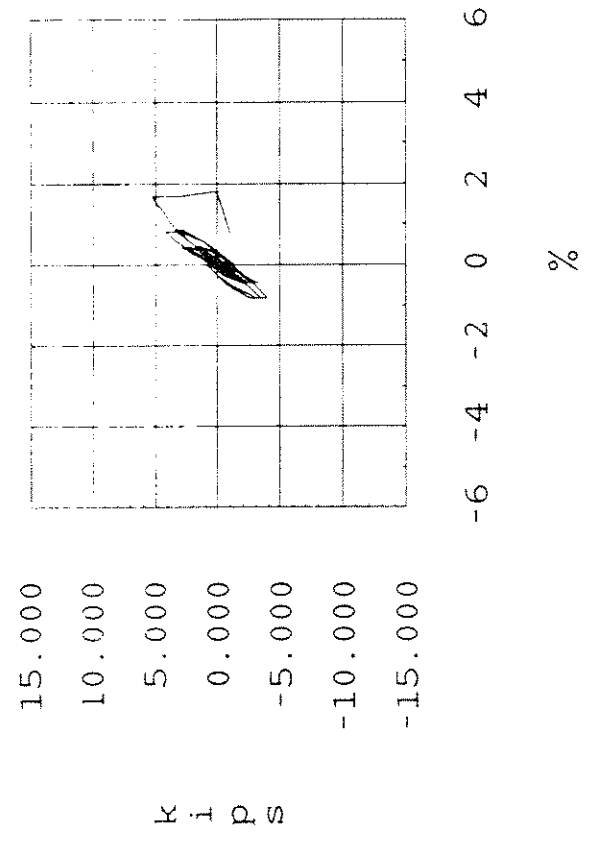


FIG. 6 - LATERAL DISPLACEMENT HISTORY AND LOADING PATTERNS



SPECIMEN AP2 EW FORCE - DRIFT



SPECIMEN AP2 NS FORCE - DRIFT

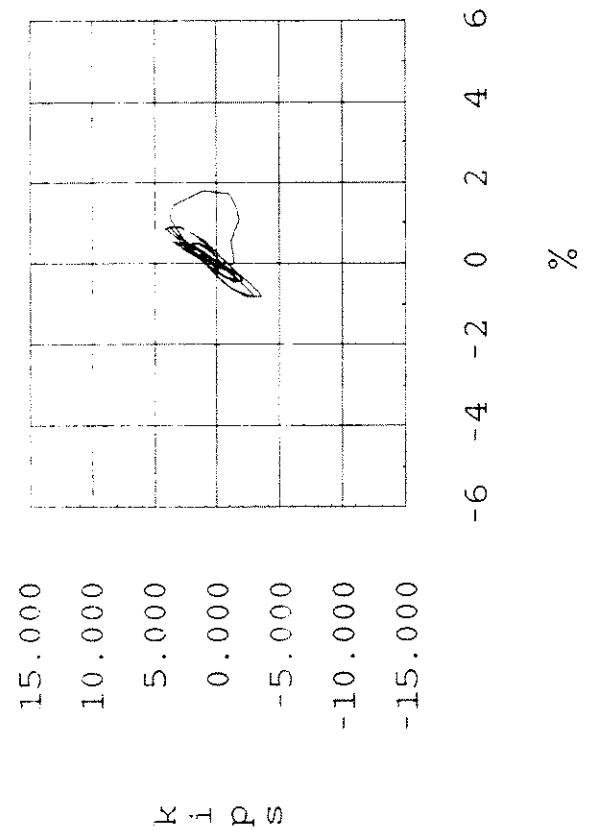
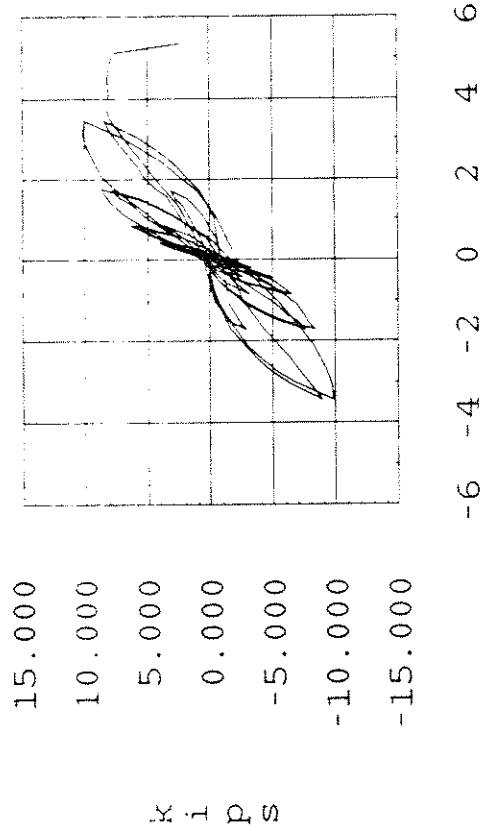
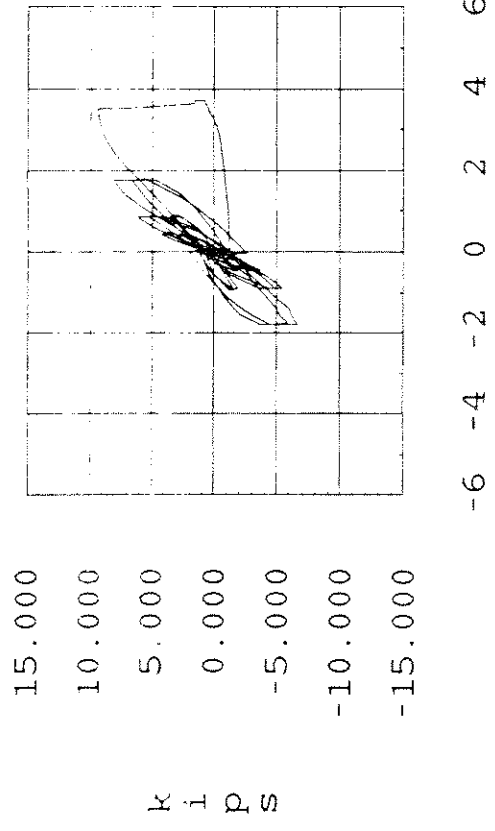


FIG. 7 - UNIAXIAL AND BIAXIAL TESTS (HIGH GRAVITY LOAD)

SPECIMEN AP3 EW FORCE - DRIFT



SPECIMEN AP4 EW FORCE - DRIFT



SPECIMEN AP4 NS FORCE - DRIFT

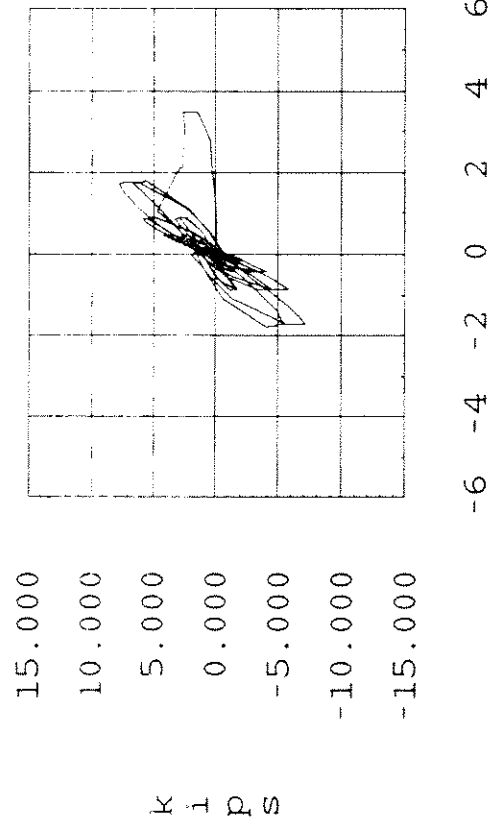
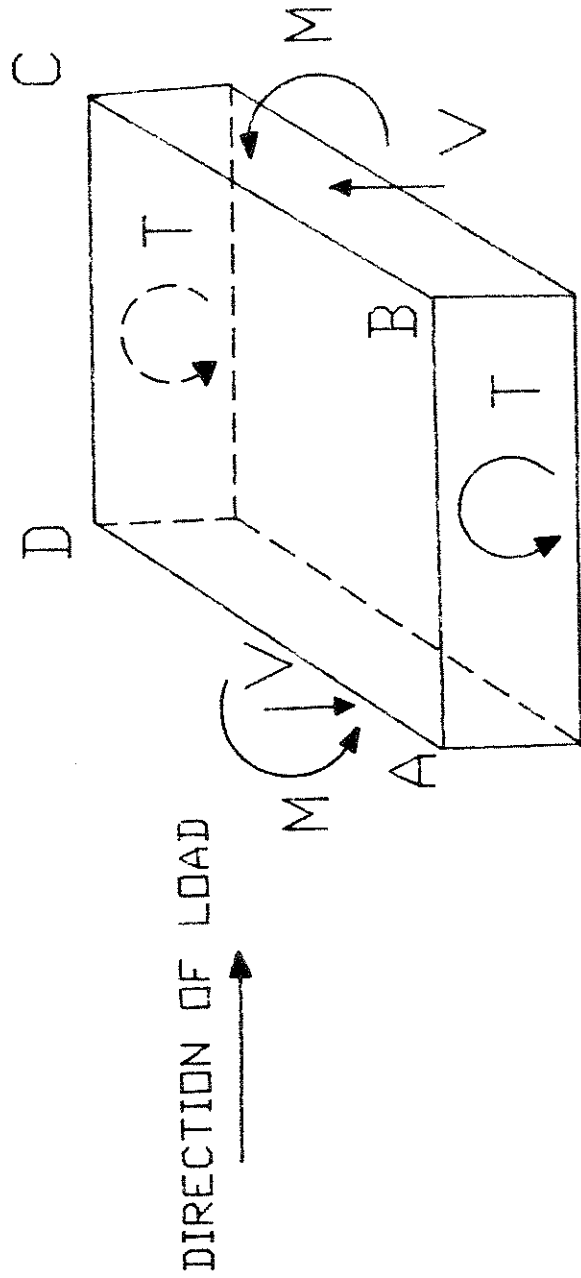
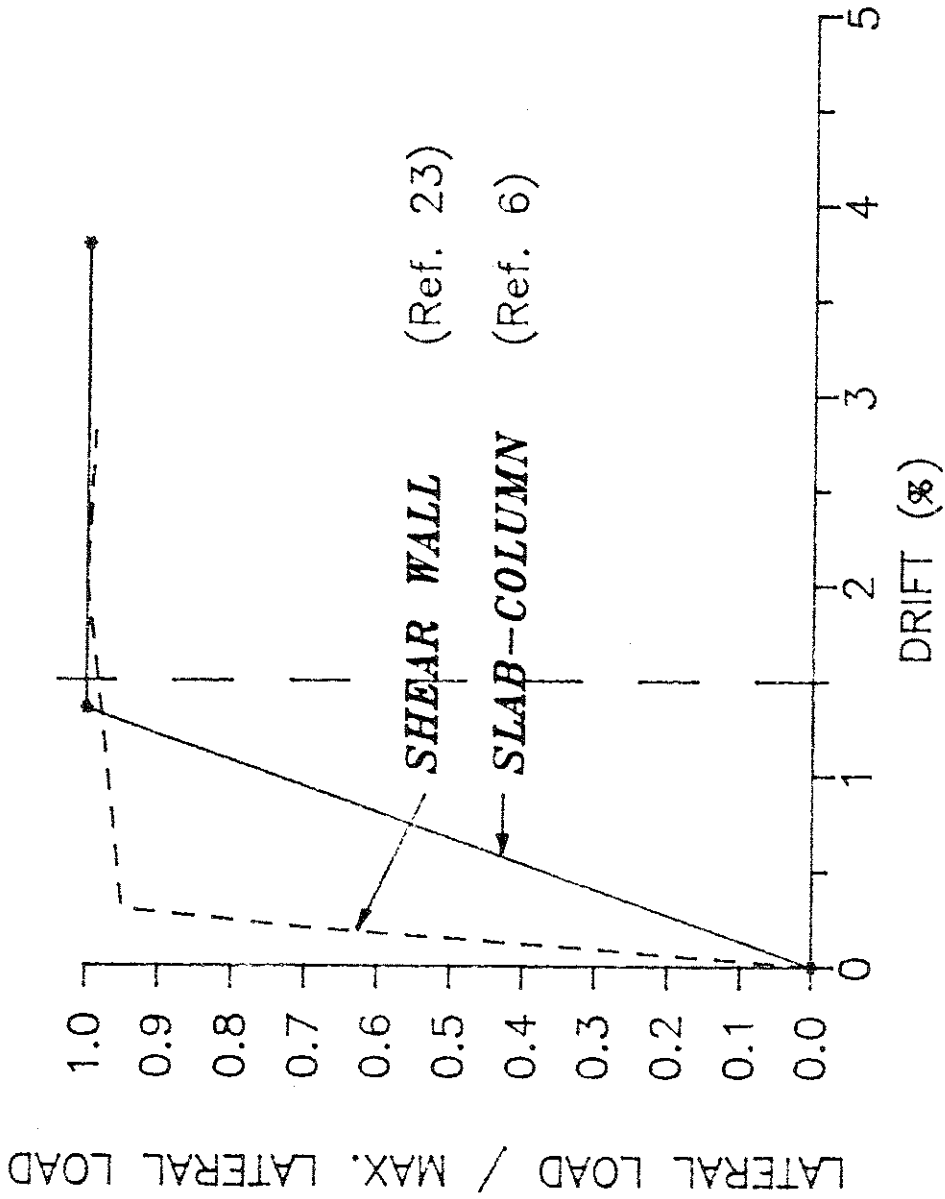


FIG. 8 - UNIAXIAL AND BIAXIAL TESTS (LOW GRAVITY LOAD)



**FIG. 9 - FORCES ON CONNECTION UNDER UNIAXIAL LOADING**





**FIG. 10 - COMPARISON OF DUCTILITY REQUIREMENTS AT 1.5% DRIFT**

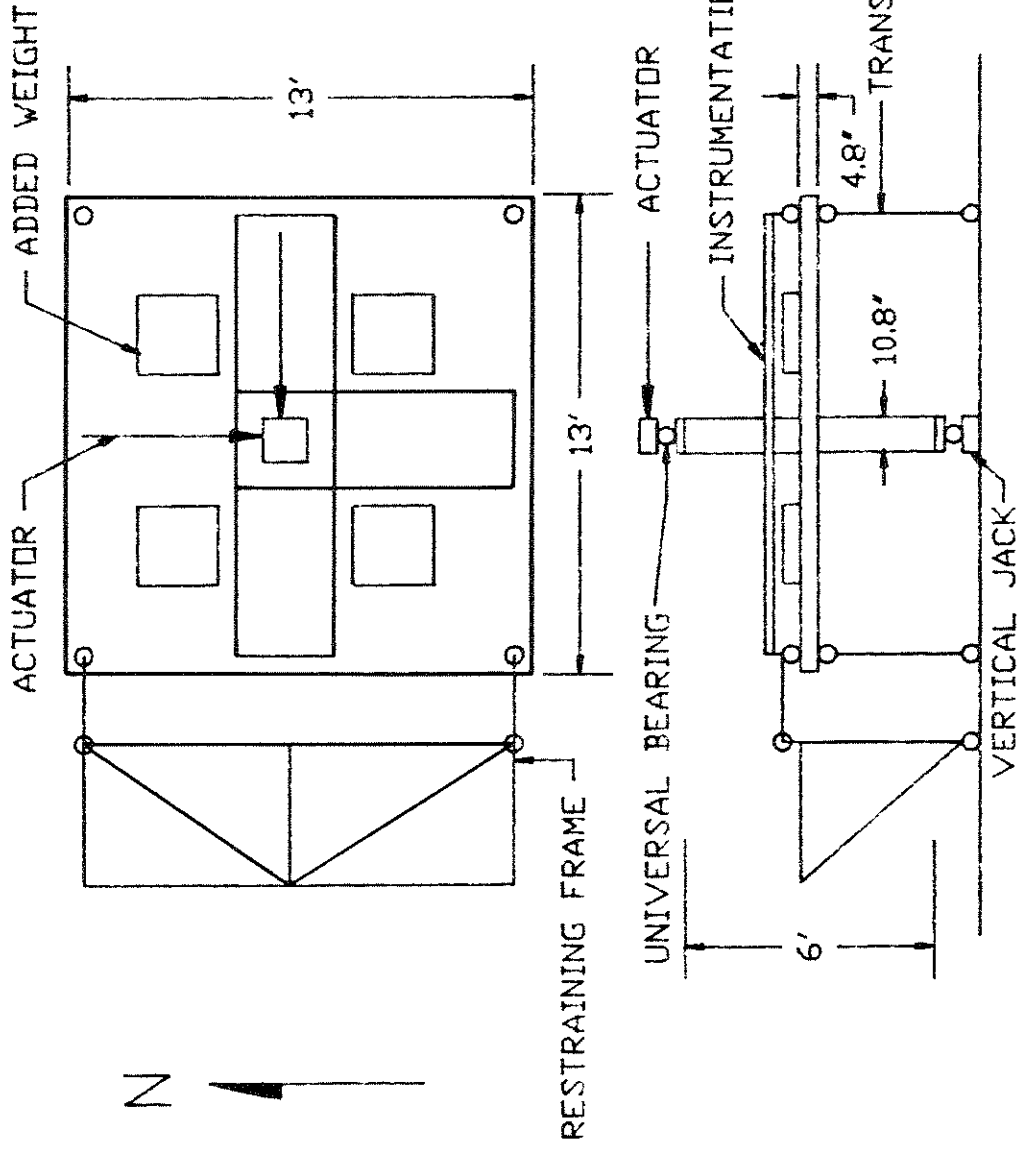


FIG. A.1 - TEST SETUP FOR BIAXIAL LOADING